ACS APPLIED MATERIALS & INTERFACES

Surfaces, Interfaces, and Applications

Photoelectrochemical biosensor for sensitive detection of soluble CD44 based on the facile construction of a polyethylene glycol/hyaluronic acid hybrid anti-fouling interface

Bobo Fan, Qi Fan, Min Cui, Tingting Wu, Jinshen Wang, Hongmin Ma, and Qin Wei

ACS Appl. Mater. Interfaces, **Just Accepted Manuscript** • DOI: 10.1021/acsami.9b06937 • Publication Date (Web): 19 Jun 2019

Just Accepted

is published by the American Chemical Society. 1155 Sixteenth Street N.W., Washington, DC 20036

Photoelectrochemical biosensor for sensitive detection of soluble CD44 based on the facile construction of a polyethylene glycol/hyaluronic acid hybrid anti-fouling interface

Bobo Fan [a], Qi Fan [a], Min Cui [a], Tingting Wu [a], Jinshen Wang [b], Hongmin Ma [a]*, Qin Wei [a]

[a] Key Laboratory of Interfacial Reaction & Sensing Analysis in Universities of Shandong, School of Chemistry and Chemical Engineering, University of Jinan, Jinan 250022, PR China.

[b] Shandong Provincial Hospital Affiliated to Shandong University, Jinan 250012, PR China.

*Corresponding Author, Fax: (86) 531 82765969; Tel: (86) 531 82760510; E-mail: mahongmin2002@126.com

Abstract: The serum level of soluble CD44 is directly associated with several clinic-pathological parameters of malignant diseases. The development of easy and cost-effective detection method for soluble CD44 is in great need for both diagnosis and treatment of cancers. In this work, a simple photoelectrochemical (PEC) method for sensitive detection of serum-soluble CD44 is proposed based on the construction of a hybrid anti-fouling coating on TiO_2 substrate. Hyaluronic acid (HA) and polyethylene glycol (PEG) are co-immobilized using a biomimetic one-step surface functionalization approach. The immobilized HA shows strong recognition abilities towards soluble CD44, and the synergistic anti-fouling effect achieved by the combination of PEG and HA improves the sensing specificity. Based on the inhibitory effect of CD44 recognition on the PEC signal of TiO_2 substrate, a PEC biosensor is developed with a wide response range and a low detection limit. The development of antibody-free biosensors may promote the application of soluble CD44 as a biomarker for diagnosis and treatment of malignant diseases.

KEYWOEDS： soluble CD44; serum biomarker; hyaluronic acid; polydopamine coating; titanium dioxide

1. INTRODUCTION

CD44 is a cellular adhesion molecule expressed on the surface of many cell types. It plays an important role in cell-cell and cell-matrix interactions. The aberrant expression of CD44 is correlated with tumor progression and metastasis. Proteolytic cleavage can produce the serum-soluble form of CD44 which can be released into circulation.[1] Recent studies have revealed that serum level of soluble CD44 is associated with several clinic-pathological parameters of cancers.[2-3] Soluble CD44 is now used as a potential biomarker for the early detection of a range of malignant diseases.[4-5] The determination of soluble CD44 in serum samples relies on the traditional ELISA assay where the enzyme and antibody-involved immunoassay is complex and expensive.[5] The development of antibody-free and cost-effective method for sensitive determination of soluble CD44 is in great need for both diagnosis and treatment of cancers.

Hyaluronic acid (HA), an anionic linear biopolymer composed of D-glucuronic acid and N-acetylglucosamine, is the main glycosaminoglycan of the extracellular matrix. CD44 is the principal cellular surface receptor for HA. The interactions between HA and CD44 are associated with many cell behaviors such as migration and proliferation.[6] While CD44 is a promising therapeutic target for metastasizing tumors, HA is widely used in targeted drug delivery, tumor diagnosis and treatment.[7-8] Based on the specific and strong affinity with CD44, HA is also used as a bio-recognition element for capture and enrichment of circulating tumor cells which are CD44-overexpressing.[9] However, there are few report about the quantitative determination of soluble CD44 based on the specific interaction between HA and CD44.[10]

Compared with other methods, such as ELISA assay and plasmonic mass spectrometry[11], photoelectrochemical (PEC) biosensing method recently has received more and more attention because it inherits and combines the advantages of photo and electrochemical methods, such as the use of simple instrument, ease of operation, and high sensitivity.[12-14] The various emerging semiconductor nanomaterials can be easily

incorporated into the sensing platform enabling a variety of novel detection strategies.[15-16] TiO_2 nanoparticles (NPs) are the most popular and successful nanomaterials for the construction of PEC biosensors due to the advantages of easy preparation and high photoelectric conversion efficiency.[17] A weakness of TiO_2 NPs for the application in biosensing is the UV response which may induce a damage to the biomolecules.[18] In previous works, we have utilized the versatile mussel-inspired polydopamine (PDA) surface chemistry for the coating of semiconductor NPs to improve the visible light response and construct a biosensing interface.[19-20] The reactivity of PDA coatings enables the facile immobilization of molecules which contain amino groups or thiols.[21-22] Furthermore, both small molecules and macromolecules can be attached to substrates using a one-step immobilization strategy.[23-24] The immobilization of HA molecules on substrates using one-pot approach has been reported.[25]

While the adhesive property of PDA enables the facile immobilization of HA molecules, it may also encounter the problem of protein fouling which is undesired for biosensing. In consider of the complicated matrix of serum samples, the fabrication of an anti-fouling sensing interface is an appealing strategy for reducing the undesired protein fouling. Polyethylene glycol (PEG) is the most widely used anti-fouling material to inhibit the adsorption of protein.[26-29] The excellent anti-fouling property of PEG originates from not only the strong hydrophilicity, which can form a hydration layer at the interface, but also the large molecular weight, which has steric repulsion effect of entropy decrease.[30] Due to the easy-to-modify structure, PEG has been successfully modified on various drug delivery systems to improve the circulation time, especially the nanocarriers.[31-33] The application of PEG in the construction of anti-fouling sensing interface seems not fully exploited, possibly because the lack of effective immobilization method on sensing interface.

In this work, PEG and HA molecules are co-immobilized on TiO_2 substrate using one-step surface functionalization to construct a PEC sensing interface (Scheme 1). While HA also possesses the high hydrophilicity and anti-fouling property, a good anti-fouling effect is expected by the combination of PEG and HA. The PDA coating

not only enables the simple immobilization of PEG and HA, but also enhance the visible light response of TiO_2 substrate. The specific recognition of soluble CD44 by the immobilized HA induces a significant decrease of the PEC signal, which enables the sensitive detection of soluble CD44. As far as we know, this is the first report about the fabrication of a PEC biosensor for soluble CD44 based on the specific interaction between HA and CD44 and the construction of PEC anti-fouling surface.

2. EXPERIMENTAL SECTION

2.1. Materials and reagents

Tris(hydroxymethyl)aminomethane (Tris), dopamine hydrochloride (DA), polyethylene glycol 4000 (PEG), hyaluronic acid (HA) and L-ascorbic acid (AA) were purchased from Shanghai Macklin Biochemical Co., Ltd. (Shanghai, China). Bovine serum albumin (BSA) was obtained from Shanghai Aladdin Biochemical Technology Co., Ltd. (Shanghai, China). CD44 was purchased from Novoprotein Scientific Inc. (Shanghai, China). Tetrabutyl titanate (TBT) and ethanol were purchased from Sinopharm Chemical Reagent Co., Ltd. All of the reagents used in the experiments are the analytical reagent grade. ITO glass supplied by China South Glass Holdings Ltd. was used as a working electrode. The ITO electrodes (2.5 cm × 0.8 cm) were continuously cleaned by ultrasound in acetone, ultra-pure water, ethanol and ultra-pure water for 30min.

2.2. Apparatus

Scanning electron microscope (SEM) images were obtained using a field emission SEM (Zeiss, Germany). High resolution transmission electron microscope (HRTEM) images were obtained using a field emission HRTEM (JEOL 1400, Japan). X-ray power diffraction (XRD) was acquired by a D8 advance X-ray diffractometer (Bruker AXS, Germany). OCA15EC (Dataphysics, Germany) was used to measure the static water contact angle at differently modified ITO electrodes. The PEC and EIS measurements were tested at room temperature on a Zahner PEC workstation

(Zennium-PP 211, Germany) using a conventional three-electrode system.

2.3. Preparation of TiO_2 NPs

TiO_2 NPs were synthesized according to the reported methods with minor modification.[34] TBT (1 mL) was firstly dissolved in 40 mL ethanol at room temperature. Then, 40 mL of ultrapure water was added dropwise to the above solution with vigorous stirring, and the mixture was stirred for 30 minutes. Next, the final suspension solution was transferred into a 100 mL Teflon-lined autoclave, and maintained at 180 ˚C for 12 h. After cooling to room temperature, the resulting product was centrifuged and rinsed with absolute ethanol and ultrapure water for several cycles to remove residual impurity. The sample obtained by vacuum drying and grinding was then stored at 4 ˚C.

2.4. Construction of the hybrid coating on TiO_2 substrate

As depicted in Scheme 1, the construction of PDA-HA or PDA-HA-PEG hybrid coatings on TiO_2 modified ITO electrodes were performed in a one-pot method. Dispersions of TiO_2 NPs in water with different concentrations were handled with ultrasonic for 30 min. And then 10 μL of TiO_2 NPs dispersion was dropped onto the conductive side of the ITO classes to maintain a PEC active area of about 0.20 cm^2 (D=0.5 cm). After drying, it was annealed in the muffle furnace at 400 ˚C for 1 h, and then cooled to room temperature. The TiO_2 modified ITO classes (ITO/TiO_2) were immersed into freshly-prepared DA solutions of 2 mg/mL buffered with Tris-HCl (pH=8.5, 0.1 M) with HA (2 mg/mL) and/or different concentrations of PEG. After 2 h, the hybrid film coated ITO/TiO_2 were rinsed by ultrapure water and used as working electrodes for the evaluation of anti-fouling property and the PEC sensing of the soluble CD44.

2.5. Characterization of the successful formation of hybrid coatings

For the confirmation of the successful formation of hybrid coatings on TiO_2 substrate, static water contact angle measurements and SEM were performed. Water

contact angle of different modified ITO electrodes was measured at standard atmospheric pressure and 50% air humidity. The prepared ITO/TiO_2, ITO/TiO_2/PDA, ITO/TiO_2/PDA-HA and ITO/TiO_2/PDA-HA-PEG electrodes were blown dry with nitrogen. Each electrode was tested three times, and the average value of the water contact angle was determined.

2.6. Investigation of the anti-fouling property of PEC sensing interface

The anti-fouling property of the fabricated sensing platform was evaluated by the EIS and PEC current changes before and after protein fouling. In a typical experiment, different modified electrodes were immersed in electrolyte solution (2.5 mM $K_3Fe(CN)_6$ and 0.1 M KCl) to establish stable EIS base responses, and then their EIS responses were recorded in the same electrolyte again after soaking in PBS (pH=7.4, 0.1 M) with 0.5 mg/mL protein (BSA, IgG, BNP or PSA) solution for 1h. In the same way, the photoelectric responses of different the modified electrodes before and after soaking in protein solution were recorded. EIS spectrum applications range in frequency from 0.1 Hz to 100 kHz. All of the photocurrent response tests were carried out in AA solutions buffered with 0.1 M PBS. The wavelength of the excitation light source is 450 nm with a bias potential of 0.0 V.

2.7. Investigation of the performance of the PEC biosensor

In order to optimize the performance of the PEC biosensor, the experimental conditions were optimized. The detailed optimization process of TiO_2 concentration, polymerization time of biomimetic film, AA concentration, PEG concentration, incubation temperature and incubation time of CD44 were in the support information (Figure S1, S2 and S3).

EIS and PEC responses of ITO/TiO_2/PDA-HA-PEG electrodes after soaking in a CD44 (10 ng/mL) solution and a mixed solution of CD44 (10 ng/mL) and BSA (0.5 mg/mL) were recorded, respectively, to investigate the selectivity of the sensor. The PEC biosensor modified with CD44 (10 ng/mL) was tested for 12 consecutive cycles of on and off light irradiations to test the signal stability of the biosensor. In addition,

in order to test the storage stability of the biosensor, the photocurrent of the biosensor modified with 10 ng/mL of CD44 was tested. And then, the photocurrent was again tested after storage for one week in an environment of 4 ˚C. Six ITO/TiO_2/PDA-HA-PEG electrodes modified with CD44 (10 ng/mL) to evaluate the fabrication reproducibility.

2.8. PEC detection of CD44

The constructed functionalized PEC biosensors were immersed into CD44 solutions with different concentrations (0.001 - 500 ng/mL) and incubated for 1 h. Then the PEC biosensors were rinsed with ultrapure water. Each concentration was tested three times, and the average value of the photocurrent was determined to build the work curve.

For real sample analysis, blood (purchased from Shandong Provincial Hospital of Traditional Chinese Medicine) was centrifuged at 3000 rpm for 10 min. The serum from the upper layer is taken out and diluted to the volume of the original blood. The content of CD44 in human serum was detected first. And then, the CD44 levels in the serum samples were measured after adding the standard CD44 solutions with different concentrations (30, 60 and 90 ng/mL).

3. RESULTS AND DISCUSSION

3.1. Characterization of TiO_2 NPs

TiO_2 nanoparticles with narrow size distribution and an average diameter of 30 nm were synthesized (Figure 1A). The EDS characterization (Figure 1B) proved that the TiO_2 NPs we synthesize has a high purity. The XRD patterns (Figure 1C) confirmed that TiO_2 NPs are of anatase form. The strong and sharp diffraction peaks confirmed the high crystallinity and purity of the materials.

3.2. Characterization of PDA-HA-PEG biomimetic films

The static water contact angle measurements scan reflect the wetting property of

the solid interface. In consider of the unique hydrophilicity of HA and PEG, the surface attachment on PDA coating was confirmed by the changes of water contact angle. The obtained water contact angles of the electrodes with different degrees of modification are shown in Figure 2 and Table S1. The water contact angles of ITO/TiO_2 electrode was 37.0° (Figure 2A). After coating with PDA, the contact angle of the surface decreased from 37.0° to 32.0° (Figure 2B), indicating moderate hydrophilicity of the PDA coatings. When HA was modified on the electrode surface, the water contact angle of the electrode surface was further reduced to 25.1° (Figure 2C). When HA and PEG were simultaneously doped onto the surface of the ITO/TiO_2/PDA electrode, the water contact angle was further decreased to 20.0° (Figure 2D). The improved hydrophilicity through the combination of HA and PEG may contribute to a better anti-fouling property.

The surface morphologies of different modified electrodes were characterized by SEM (Figure 3). It can be seen from Figure 3A that TiO_2 NPs agglomerated into microspheres attached to the ITO electrode surface. As shown in Figure 3B, there is a PDA coating on the surface of ITO/TiO_2/PDA electrode. It can be seen from the inset of Figure 3B that that the PDA coating is composed of PDA pellets. With the introduction of high hydrophilic polymers HA (Figure 3C) and PEG (Figure 3D), the surface of the electrode gradually becomes smooth.

3.3. Investigation of the influence of PDA-HA-PEG hybrid coating on the photoelectric response of biosensor

In order to study the influence of PDA-HA-PEG hybrid coating of TiO_2, the photocurrent responses of ITO/TiO_2 electrode before and after PDA-HA-PEG biomimetic film modification was recorded. As shown in Figure 4, the photocurrent of ITO/TiO_2/PDA-HA-PEG electrode (30.79 μA, red curve) is much higher than that of ITO/TiO_2 electrode (9.83 μA, black curve). The results show that PDA-HA-PEG biomimetic film can improve the visible light response of the ITO/TiO_2 electrode.

3.4. Investigation of anti-fouling property of PEC biosensor

In order to evaluate the anti-fouling property of the PEC biosensor, EIS (Figure 5A, B and C) and photocurrent responses (Figure 5D, E and F) of different modified electrodes before (black curve) and after (red curve) soaking in BSA solution were recorded to compared the difference. As shown in the Figure 5, the impedance spectrum includes the semicircle part with higher frequency and the linear part with lower frequency. The semicircle part is equivalent to the electron transfer resistance (R_{et}), which reflects the limited diffusion of the redox probe in the multilayer system. As shown in Figure 5A, compared with the R_{et} value of ITO/TiO_2/PDA electrode before soaking in BSA solution, the R_{et} value was significantly increased after soaking in BSA solution, indicating an apparent protein fouling. Although the modification of the PDA coating increases the hydrophilicity of the ITO/TiO_2 electrode, it can be coupled with the protein due to the adhesive of the PDA coating, which makes the ITO/TiO_2/PDA electrode exhibits poor anti-fouling property. A large amount of BSA is adsorbed on the surface of ITO/TiO_2/PDA electrode, which hinders electron transfer and leads to the increase of the R_{et} value. The incorporation of HA and PEG into PDA coatings also induces an increase of R_{et} value. This may be due to the HA and PEG, as non-conductive polymers, can hinder electron transfer to some extent.[26] The PDA films have been reported possess the semi-permeability.[35] However, the hybrid films show enhanced protein anti-fouling effect. Compared with ITO/TiO_2/PDA electrode, the R_{et} value of ITO/TiO_2/PDA electrode (Figure 5B) changes little, which proves that the introduction of HA enhances the anti-fouling ability of the surface of the ITO/TiO_2/PDA electrode. Comparatively, less obvious change of R_{et} value was obtained for ITO/TiO_2/PDA-HA-PEG electrode (Figure 5C), demonstrating the synergistic anti-fouling effect of HA and PEG. This may be because the surface of the ITO/TiO_2/PDA-HA-PEG electrodes has stronger hydrophilicity and the PEG has a steric repulsion effect of entropy decrease, which can reduce the protein adsorption on the surfaces.[36]

The anti-fouling effect can also be monitored by the change of PEC currents. We have previously reported the enhancement effect of PDA coatings on PEC currents. Although the incorporation of HA and PEG into PDA coatings increase the R_{et} value,

an obvious enhancement effect on PEC currents were achieved for hybrid coating. This may be because the introduction of HA and PEG inhibits the agglomeration of dopamine, making the PDA coating smoother, which increases the absorption of light by TiO_2.[25, 37] The inhibitory effect of protein attachment on PEC currents have been well demonstrated by the reported PEC biosensors. As shown in Figure 5D, as expected, the photocurrent of ITO/TiO_2/PDA electrode after soaking in BSA solution was significantly reduced. BSA adsorbed on the ITO/TiO_2/PDA electrode hindered the surface reaction between AA and the photo-induced holes, which will lead to the decrease of the photocurrent. The photocurrent of the ITO/TiO_2/PDA-HA electrode (Figure 5E) decreased slightly after immersion in BSA solution, compared with the ITO/TiO_2/PDA electrode. In consistent with the EIS measurements, ITO/TiO_2/PDA-HA-PEG electrode shows better anti-fouling effect toward the adsorption of BSA (Figure 5F).

In order to verify the anti-fouling property of PEC biosensor towards proteins, a common interfering serum protein, IgG, and two common protein biomarkers usually present in serum, BNP and PSA, were further used as biofouling agents. Based on the EIS and PEC evaluations, the hybrid film coated PEC biosensor ITO/TiO_2/PDA-HA-PEG also shows good anti-fouling property towards IgG (Figure S5A and D), BNP (Figure S5B and E)and PSA(Figure S5C and F).

While the non-specific adsorption of protein can be effectively inhibited by the incorporation of PEG, the recognition ability of HA towards soluble CD44 is still in demand. As the same to the investigation method of protein fouling, the recognition abilities of the fabricated PEC electrodes were also evaluated by the EIS and photocurrent measurements. The soaking of ITO/TiO_2/PDA-HA electrode into a CD44 solution (10 ng/mL) induces significant increase of R_{et} value (Figure 6A) and decrease of photocurrent (Figure 6C), which can be explained by the attachment of CD44 on the electrode. The similar changes of R_{et} value (Figure 6B) and photocurrent (Figure 6D) for the soaking of ITO/TiO_2/PDA-HA-PEG electrode into a same solution indicate that the recognition ability of HA is well retained after the introduction of PEG.

3.5. Characterization of the performance of PEC biosensors

The sensing performance of the fabricated electrode towards the target protein can be further demonstrated by the recognition specificity for mixed solutions. The EIS (Figure 7A) and photocurrent responses (Figure 7B) of ITO/TiO_2/PDA-HA-PEG electrode for a CD44 solution and a mixed solution of CD44 (10 ng/mL) and BSA were recorded. It can be seen that the presence of BSA (50 times in concentration) has little influence on the recognition of CD44. A balance between the protein anti-fouling and target protein recognition has been achieved by the proposed hybrid coating method.

The signal stability and fabrication reproducibility are two major indicators affecting the performance and usability of the PEC biosensor. It can be seen from Figure 8A that the photocurrent was relatively stable, and the relative standard deviation (RSD) of 12 consecutive cycles was 0.76%. In addition, the photocurrent of the biosensor after storage for one week decreased by only 5.7%. The RSD of the six different biosensors was 1.2% (Figure 8B). The results showed that the proposed biosensor had good stability and reproducibility.

3.6. Quantitative determination of soluble CD44

With the best conditions, the constructed PEC biosensor was used to determine CD44 in several standard solutions with different concentrations and the photocurrent response of PEC biosensor reflected the concentration of CD44 was recorded. As shown in Figure 9A, as the concentration of CD44 increased, the photocurrent gradually decreased. Therefore this PEC method can be used to quantitatively detect CD44. Figure 9B showed that there is a good linear relationship between the photocurrent and the logarithm value of CD44 concentration in the range from 0.005 ng/mL to 500 ng/mL. The linear equation was I = -3.28 lg$c$ +20.67 (R^2=0.998), and the detection limit (S/N=3) was 0.44 pg/mL. Compared to other methods, the sensor has a wide detection range and a low detection limit.[38-41]

3.7. Real sample analysis

In order to analyze the application property of the constructed PEC biosensor in the actual analysis, the recovery of different concentrations of CD44 in the serum samples were tested. As shown in Table 1, the recovery of different concentrations of CD44 ranged from 100.5% to 102.95%, and the RSD ranged from 2.04% to 2.35%.

4. CONCLUSIONS

In summary, the HA and PEG were successfully co-immobilized on TiO_2 substrate using one-step PDA surface functionalization to construct a PEC biosensor for high sensitivity detection of CD44. The presence of PDA greatly increases the photoelectric response of TiO_2. At the same time, due to the good anti-fouling property of PEG, the introduction of PEG into the surface of the PEC biosensor makes the PEC biosensor also have excellent anti-fouling property while maintaining the sensitive detection of CD44. The constructed PEC biosensor had a wide assay range from 0.005 ng/mL to 500 ng/mL and a low detection limit of 0.44 pg/mL. Due to high sensitivity and anti-fouling property, the platform has broad application prospects in the development of biosensors and clinical application of biosensors.

Supporting Information

Supporting materials include the optimization conditions of PEC biosensor fabrication and sensing, the static water contact angles values of the different electrodes, the stability test of ITO/TiO_2 electrode, the Nyquist plots of EIS and photocurrent responses of the PEC biosensor before and after soaking in IgG, BNP and PSA solution, the R_{et} value and photocurrent of the different electrodes and the comparison of different approaches for CD44.

AUTHOR INFORMATION

Corresponding Author

*Fax: (86) 531 82765969; Tel: (86) 531 82760510; E-mail: mahongmin2002@126.com

Notes

The authors declare no competing financial interest.

Acknowledgements

This study was financially supported by the National Natural Science Foundation of China (21675063), the National Key Scientific Instrument and Equipment Development Project of China (No. 21627809), and Jinan Scientific Research Leader Workshop Project (2018GXRC024).

REFERENCES

(1) Rokhlin, O. W.; Cohen, M. B. Soluble Forms of CD44 and CD54 (ICAM-1) Cellular Adhesion Molecules are Released by Human Prostatic Cancer Cell Lines. *Cancer Lett.* **1996**, *107* (1), 29-35.

(2) Sebastian, M.; Axel, Z. H.; Dirk Otto, W.; Stefan, S.; Markus, J. G.; Gerald, G.; Elmar, S. Increased Soluble CD44 Concentrations are Associated with Larger Tumor Size and Lymph Node Metastasis in Breast Cancer Patients. *J. Cancer. Res. Clin. Oncol.* **2008**, *134* (11), 1229-1235.

(3) Zeimet, A. G.; Widschwendter, M.; Uhl-Steidl, M.; Müller-Holzner, E.; Daxenbichler, G.; Marth, C.; Dapunt, O. High Serum Levels of Soluble CD44 Variant Isoform V5 are Associated with Favourable Clinical Outcome in Ovarian Cancer. *Brit. J. Cancer.* **1997**, *76* (12), 1646-1651.

(4) Franzmann, E. J.; Reategui, E. P.; Pedroso, F.; Pernas, F. G.; Karakullukcu, B. M.; Carraway, K. L.; Hamilton, K.; Singal, R.; Goodwin, W. J. Soluble CD44 is A Potential Marker for the Early Detection of Head and Neck Cancer. *Cancer. Epidem. Biomar.* **2007**, *16* (7), 1348-1355.

(5) Masson, D.; Denis, M. G.; Denis, M.; Blanchard, D.; Loirat, M. J.; Cassagnau, E.; Lustenberger, P. Soluble CD44: Quantification and Molecular Repartition in Plasma of Patients with Colorectal Cancer. *Brit. J. Cancer.* **1999**, *80* (12), 1995-2000.

(6) Ahrens, T.; Sleeman, J. P.; Schempp, C. M.; Howells, N.; Hofmann, M.; Ponta, H.; Herrlich, P.; Simon, J. C. Soluble CD44 Inhibits Melanoma Tumor Growth by Blocking Cell Surface CD44 Binding to Hyaluronic Acid. *Oncogene* **2001**, *20* (26), 3399-3408.

(7) Dreaden, E. C.; Morton, S. W.; Shopsowitz, K. E.; Jae-Hyeok, C.; Zhou, J. Deng.; Nam-Joon, C.; Hammond, P. T. Bimodal Tumor-Targeting from Microenvironment Responsive Hyaluronan Layer-by-Layer (LbL) Nanoparticles. *ACS Nano* **2014**, *8* (8), 8374-8382.

(8) Ganesh, S.; Iyer, A. K.; Morrissey, D. V.; Amiji, M. M. Hyaluronic Acid Based Self-assembling Nanosystems for CD44 Target Mediated SiRNA Delivery to Solid Tumors. *Biomaterials* **2013**, *34* (13), 3489-3502.

(9) Wang, M.; Xiao, Y.; Lin, L.; Zhu, X.; Du, L.; Shi, X. A Microfluidic Chip Integrated with Hyaluronic Acid-Functionalized Electrospun Chitosan Nanofibers for Specific Capture and Nondestructive Release of CD44-Overexpressing Circulating Tumor Cells. *Bioconjugate. Chem.* **2018**, *29* (4), 1081-1090.

(10) Huang, Y.; Yao, X.; Zhang, R.; Ouyang, L.; Jiang, R.; Liu, X.; Song, C.; Zhang, G.; Fan, Q.;

Wang, L. Cationic Conjugated Polymer/Fluoresceinamine-Hyaluronan Complex for Sensitive Fluorescence Detection of CD44 and Tumor-Targeted Cell Imaging. *ACS Appl. Mater. Interfaces* **2014**, *6* (21), 19144-1090.

(11) Wu, S.; Qian, L.; Huang, L.; Sun, X.; Su, H.; Gurav, D. D.; Jiang, M.; Cai, W.; Qian, K. A Plasmonic Mass Spectrometry Approach for Detection of Small Nutrients and Toxins. *Nano-Micro Lett.* **2018**, *10* (03), 155-163.

(12) Li, R.; Tu, W.; Wang, H.; Dai, Z. Near-Infrared Light Excited and Localized Surface Plasmon Resonance-Enhanced Photoelectrochemical Biosensing Platform for Cell Analysis. *Anal. Chem.* **2018**, *90* (15), 9403-9409.

(13) Wang, B.; Mei, L. P.; Ma, Y.; Xu, Y. T.; Ren, S. W.; Cao, J. T.; Liu, Y. M.; Zhao, W. W. Photoelectrochemical-Chemical-Chemical Redox Cycling for Advanced Signal Amplification: Proof-of-Concept Toward Ultrasensitive Photoelectrochemical Bioanalysis. *Anal. Chem.* **2018**, *90* (21), 12347-12351.

(14) Wang, C.; Li, Y.; Xu, E.; Zhou, Q.; Chen, J.; Wei, W.; Liu, Y.; Liu, S. A Label-Free PFP-Based Photoelectrochemical Biosensor for Highly Sensitive Detection of PARP-1 Activity. *Biosens. Bioelectron.* **2019**, *138*, 111308.

(15) Zhang, N.; Ruan, Y.; Zhang, L.; Zhao, W.; Xu, J.; Chen, H. Nanochannels Photoelectrochemical Biosensor. *Anal. Chem.* **2018**, *90* (3) : 2341-2347.

(16) Zhou, Q.; Xue, H.; Zhang, Y.; Lv, Y.; Li, H.; Liu, S.; Shen, Y.; Zhang, Y. Metal-Free All-Carbon Nanohybrid for Ultrasensitive Photoelectrochemical Immunosensing of Alpha-Fetoprotein. *ACS Sensors* **2018**, *3* (7), 1385-1391.

(17) Chang, Y. S.; Choi, M.; Baek, M.; Hsieh, P. Y.; Yong, K.; Hsu, Y. J. CdS/CdSe Co-Sensitized Brookite H: TiO_2 Nanostructures: Charge Carrier Dynamics and Photoelectrochemical Hydrogen Generation. *Appl. Catal. B-Environ.* **2018**, *225*: 379-385.

(18) Shu, J.; Qiu, Z.; Lv, S.; Zhang, K.; Tang, D. Plasmonic Enhancement Coupling with Defect-Engineered TiO_2-x: A Mode for Sensitive Photoelectrochemical Biosensing. *Anal. Chem.* **2018**, *90* (4), 2425-2429.

(19) Ma, H.; Yan, T.; Zhang, Y.; Gao, P.; Pang, X.; Du, B.; Wei, Q. A Biomimetic Mussel-Inspired Photoelectrochemical Biosensing Chip for the Sensitive Detection of CD146. *Analyst* **2015**, *140* (15), 5019-5022.

(20) Ma, H.; Fan, Q.; Fan, B.; Zhang, Y.; Fan, D.; Wu, D.; Wei, Q. Formation of Homogeneous Epinephrine-Melanin Solutions to Fabricate Electrodes for Enhanced Photoelectrochemical Biosensing. *Langmuir* **2018**, *34* (26), 7744-7750.

(21) Lee, H.; Dellatore, S. M.; Miller, W. M.; Messersmith, P. B. Mussel-Inspired Surface Chemistry for Multifunctional Coatings. *Science* **2007**, *318* (5849), 426-430.

(22) Lee, H.; Rho, J.; Messersmith, P. B. Facile Conjugation of Biomolecules onto Surfaces via Mussel Adhesive Protein Inspired Coatings. *Adv. Mater.* **2010**, *21* (4), 431-434.

(23) Kang, S. M.; Hwang, N. S.; Yeom, J.; Park, S. Y.; Messersmith, P. B.; Choi, I. S.; Langer, R.; Anderson, D. G.; Lee, H. One-Step Multipurpose Surface Functionalization by Adhesive Catecholamine. *Adv. Funct. Mater.* **2012**, *22* (14), 2949-2955.

(24) Zhang, Y.; Panneerselvam, K.; Ogaki, R.; Hosta-Rigau, L.; van-der, Westen. R.; Jensen, B. E.; Teo, B. M.; Zhu, M.; Städler, B. Assembly of Poly(dopamine)/Poly(N-isopropylacrylamide) Mixed Films and their Temperature-Dependent Interaction with Proteins, Liposomes, and Cells. *Langmuir* **2013**, *29* (32), 10213-10222.

(25) Huang, R.; Liu, X.; Ye, H.; Su, R.; Qi, W.; Wang, L.; He, Z. Conjugation of Hyaluronic Acid onto Surfaces via the Interfacial Polymerization of Dopamine to Prevent Protein Adsorption. *Langmuir* **2015**, *31* (44), 12061-12070.

(26) Hui, N.; Sun, X.; Niu, S.; Luo, X. PEGylated Polyaniline Nanofibers: Antifouling and Conducting Biomaterial for Electrochemical DNA Sensing. *ACS Appl. Mater. Interfaces* **2017**, *9* (3), 2914-2923.

(27) Cui, M.; Song, Z.; Wu, Y.; Guo, B.; Fan, X.; Luo, X. A Highly Sensitive Biosensor for Tumor Maker Alpha Fetoprotein Based on Poly(ethylene glycol) Doped Conducting Polymer PEDOT. *Biosens. Bioelectron.* **2016**, *79*, 736-741.

(28) Liu, N.; Xu, Z.; Morrin, A.; Luo, X. Low Fouling Strategies for Electrochemical Biosensors Targeting Disease Biomarkers. *Anal. Methods* **2019**, *11* (6), 702-711.

(29) Wang, G.; Xu, Q.; Liu, L.; Su, X.; Lin, J.; Xu, G.; Luo, X. Mixed Self-Assembly of Polyethylene Glycol and Aptamer on Polydopamine Surface for Highly Sensitive and Low-Fouling Detection of Adenosine Triphosphate in Complex Media. *ACS Appl. Mater. Interfaces* **2017**, *9* (36), 31153-31160.

(30) Indrani, B.; Pangule, R. C.; Kane, R. S. Antifouling Coatings: Recent Developments in the Design of Surfaces that Prevent Fouling by Proteins, Bacteria, and Marine Organisms. *Adv. Mater.* **2011**, *23* (6), 690-718.

(31) Han, X.; Li, Z.; Sun, J.; Luo, C.; Li, L.; Liu, Y.; Du, Y.; Qiu, S.; Ai, X.; Wu, C. Stealth CD44-Targeted Hyaluronic Acid Supramolecular Nanoassemblies for Doxorubicin Delivery: Probing the Effect of Uncovalent Pegylation Degree on Cellular Uptake and Blood Long Circulation. *J. Control. Release* **2015**, *197*, 29-40.

(32) Ju, Y.; Cui, J.; Sun, H.; Müllner, M.; Dai, Y.; Guo, J.; Bertleff-Zieschang, N.; Suma, T.; Richardson, J. J.; Caruso, F. Engineered Metal-Phenolic Capsules Show Tunable Targeted Delivery to Cancer Cells. *Biomacromolecules* **2016**, *17* (6), 2268-2276.

(33) Otsuka, H.; Nagasaki, Y.; Kataoka, K. PEGylated Nanoparticles for Biological and Pharmaceutical Applications. *Adv. Drug. Deliver. Rev.* **2012**, *64*, 246-255.

(34) Zhao, L.; Lei, Z.; Song, W.; Qin, Z.; Zeng, D.; Xie, C., In Situ Synthesis of C-TiO_2/g-C_3N_4 Heterojunction Nanocomposite as Highly Visible Light Active Photocatalyst Originated from Effective Interfacial Charge Transfer. *Appl. Catal. B-Environ.* **2017**, *202*, 489-499.

(35) Li, R.; Liu, X.; Qiu, W.; Zhang, M. In Vivo Monitoring of H_2O_2 with Polydopamine and Prussian Blue-coated Microelectrode. *Anal. Chem.* **2016**, *88* (15), 7769-7776.

(36) Ma, H.; Hyun, J.; Stiller, P.; Chilkoti, A. "Non-fouling" Oligo (Ethylene Glycol)-Functionalized Polymer Brushes Synthesized by Surface-Initiated Atom Transfer Radical Polymerization. *Adv. Mater.* **2004**, *16* (4), 338-341.

(37) Chang, C. C.; Kolewe, K. W.; Li, Y.; Kosif, I.; Freeman, B. D.; Carter, K. R.; Schiffman, J. D.; Emrick, T. Underwater Superoleophobic Surfaces Prepared from Polymer Zwitterion/Dopamine Composite Coatings. *Adv. Mater. Interfaces* **2016**, *3* (6), 1500521.

(38) Zhao, J.; Tang, Y.; Cao, Y.; Chen, T.; Chen, X.; Mao, X.; Yin, Y.; Chen, G. Amplified electrochemical detection of surface biomarker in breast cancer stem cell using self-assembled supramolecular nanocomposites. *Electrochimica Acta* **2018,** *283*, 1072-1078.

(39) Huang, Y.; Yao, X.; Zhang, R.; Ouyang, L.; Jiang, R.; Liu, X.; Song, C.; Zhang, G.; Fan, Q.; Wang, L. Cationic Conjugated Polymer/Fluoresceinamine-Hyaluronan Complex for Sensitive Fluorescence Detection of CD44 and Tumor-Targeted Cell Imaging. *ACS Appl. Mater. Interfaces* **2014,** *6* (21), 19144-19153.

(40) Zhang, R.; Rejeeth, C.; Xu, W.; Zhu, C.; Liu, X.; Wan, J.; Jiang, M.; Qian, K. Label-Free

Electrochemical Sensor for CD44 by Ligand-Protein Interaction. *Anal. Chem.* **2019**, *91* (11), 7078-7085.

(41) Rejeeth, C.; Pang, X.; Zhang, R.; Xu, W.; Sun, X.; Liu, B.; Lou, J.; Wan, J.; Gu, H.; Yan, W. Extraction, Detection, and Profiling of Serum Biomarkers Using Designed Fe_3O_4@SiO_2@HA Core–Shell Particles. *Nano Res.* **2018,** *11* (1), 68-79.

FIGURE CAPTIONS

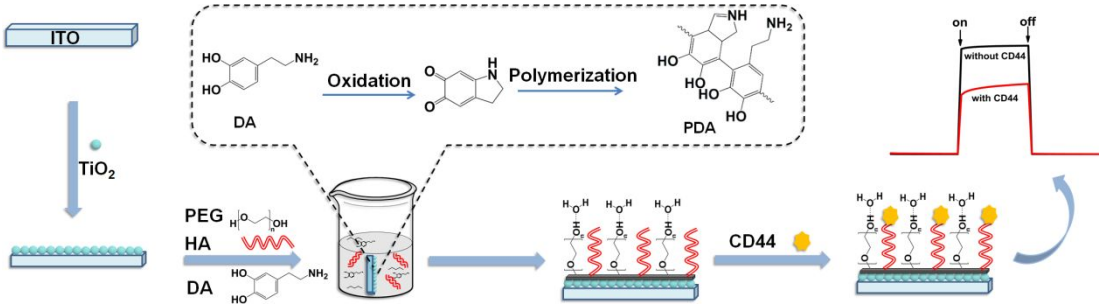

Scheme 1. Schematic representation of the fabrication of a PEC biosensor for soluble CD44 detection based on a one-step co-immobilization approach.

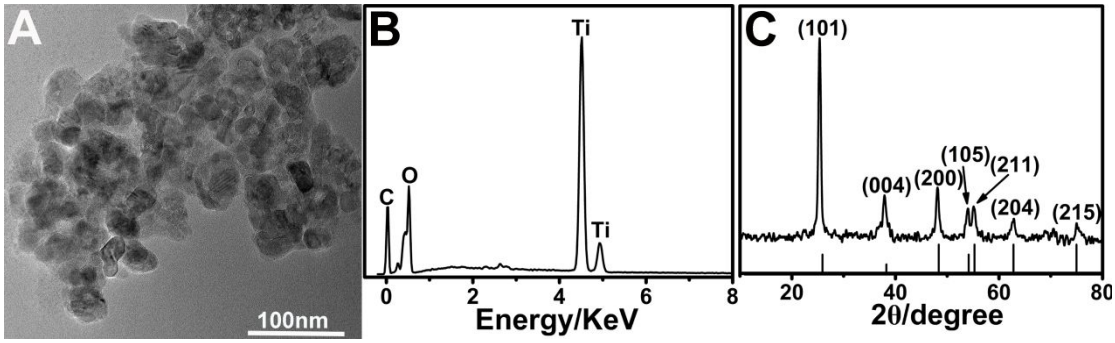

Figure 1. The TEM image (A), EDS pattern (B) and XRD pattern (C) of the TiO_2 NPs.

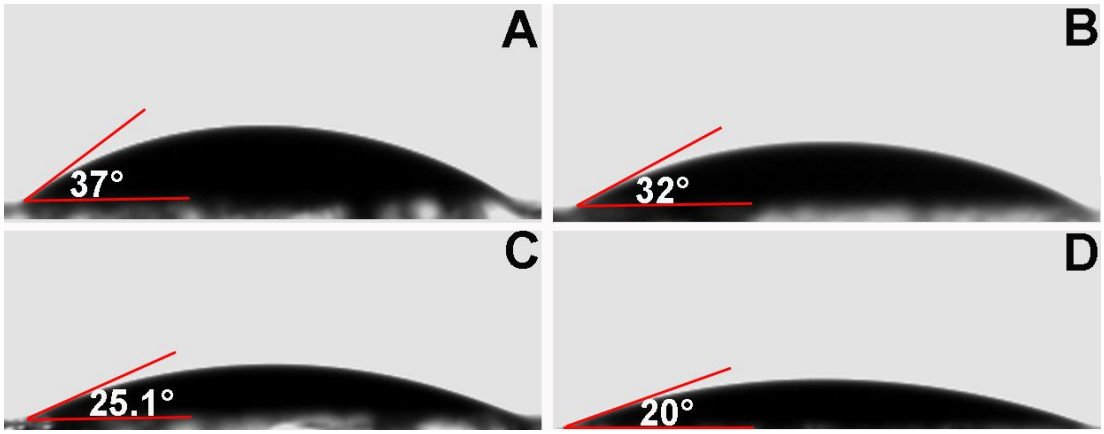

Figure 2. Static water contact angles of the surfaces of differently modified ITO electrodes: (A) ITO/TiO_2, (B) ITO/TiO_2/PDA, (C) ITO/TiO_2/PDA-HA and (D) ITO/TiO_2/PDA-HA-PEG.

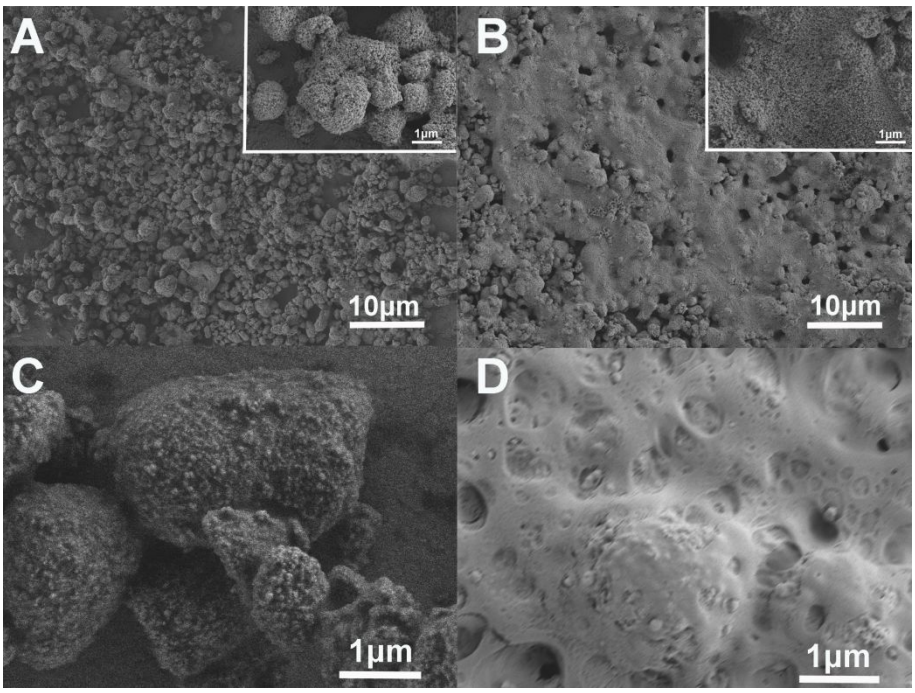

Figure 3. The SEM images of ITO/TiO_2 (A), ITO/TiO_2/PDA (B), ITO/TiO_2/PDA-HA (C) and ITO/TiO_2/PDA-HA-PEG (D) (The inset in Figure A is an SEM image of ITO/TiO_2; the inset in Figure B is an SEM image of ITO/TiO_2/PDA).

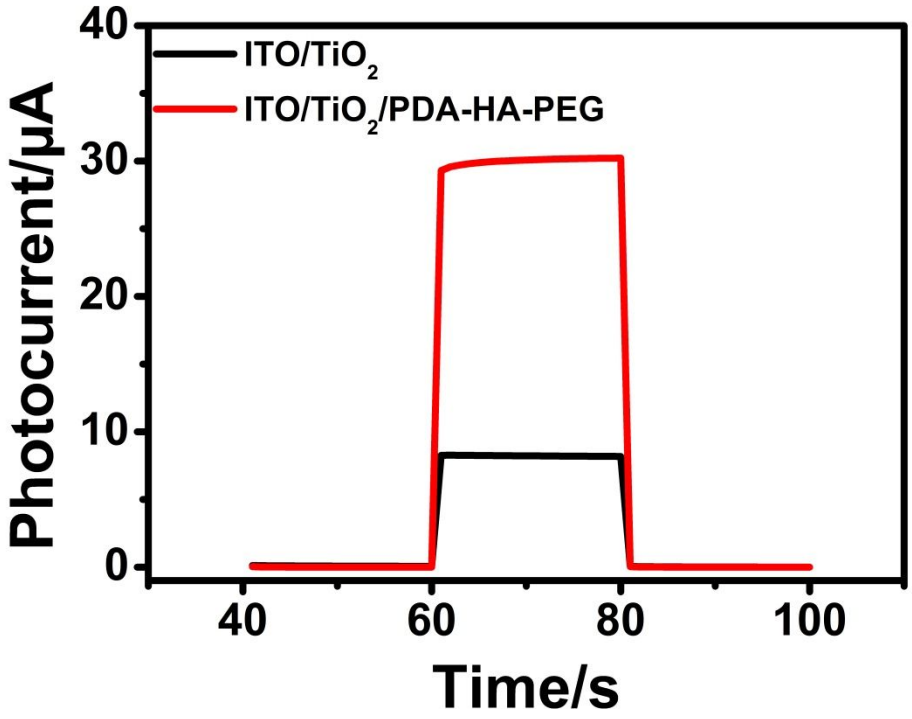

Figure 4. Photocurrent responses of the ITO/TiO_2 electrode and ITO/TiO_2/PDA-HA-PEG electrode

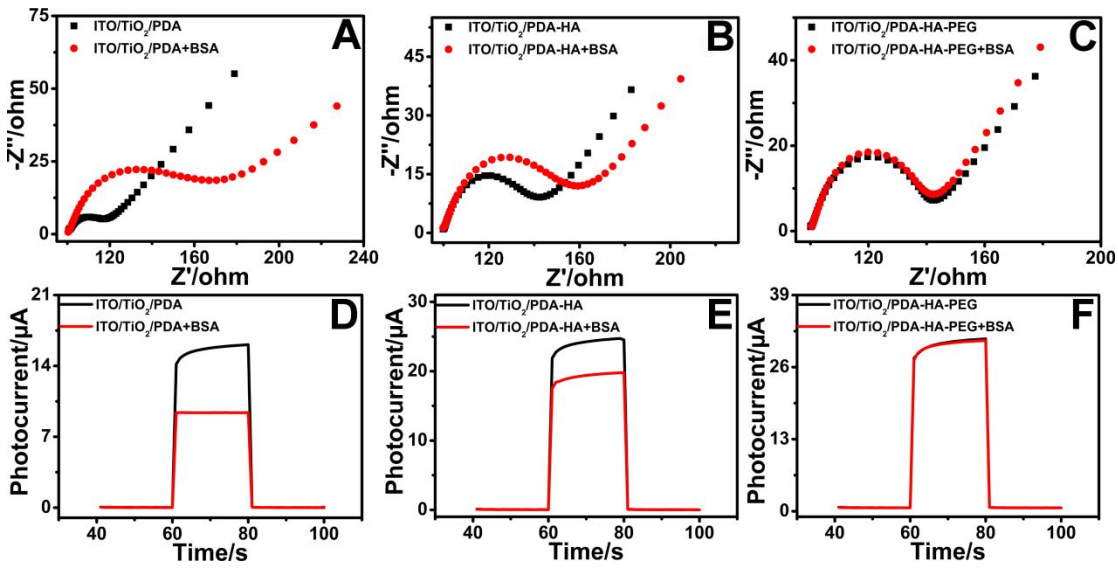

Figure 5. Nyquist plots of EIS and photocurrent responses of the different modified electrodes before (black curve) and after (red curve) soaking in BSA solution (0.5 mg/mL): (A and D) ITO/TiO_2/PDA, (B and E) ITO/TiO_2/PDA-HA, (C and F) ITO/TiO_2/PDA-HA-PEG.

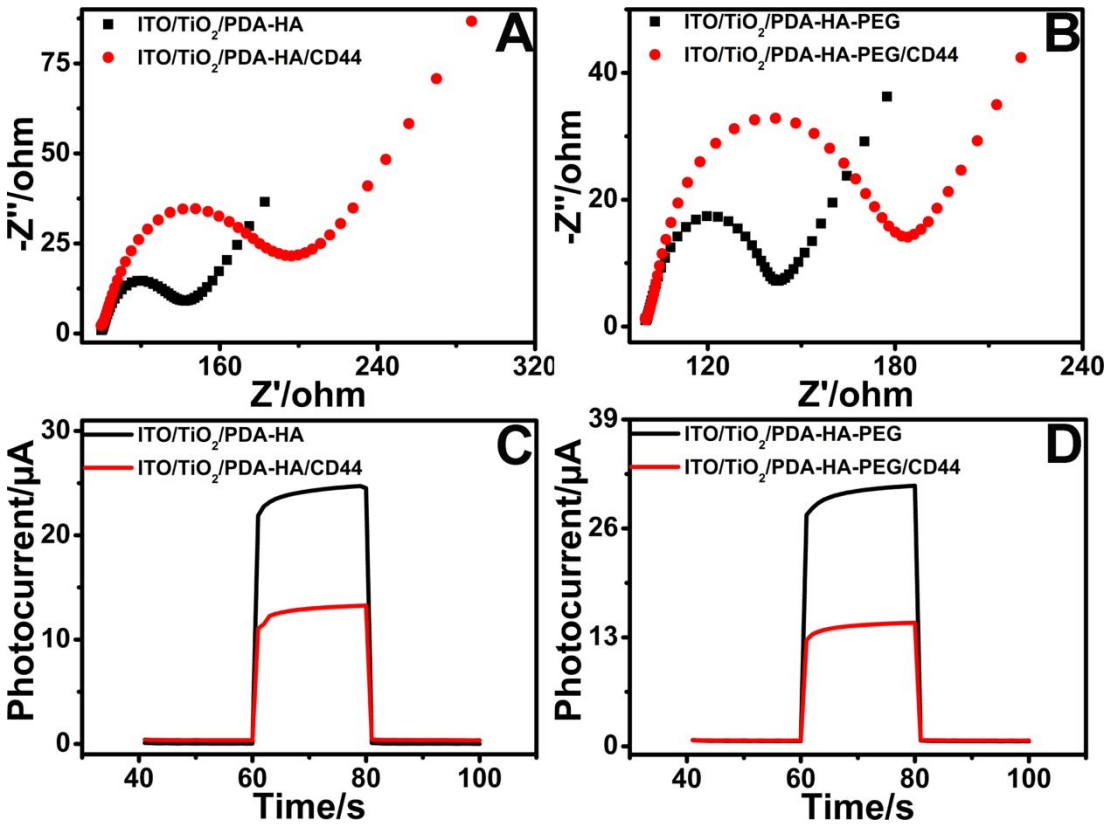

Figure 6. Nyquist plots of EIS and photocurrent responses of the different modified electrodes before (black curve) and after (red curve) soaking in CD44 solution (10 ng/mL): (A and C) ITO/TiO_2/PDA-HA, (B and D) ITO/TiO_2/PDA-HA-PEG.

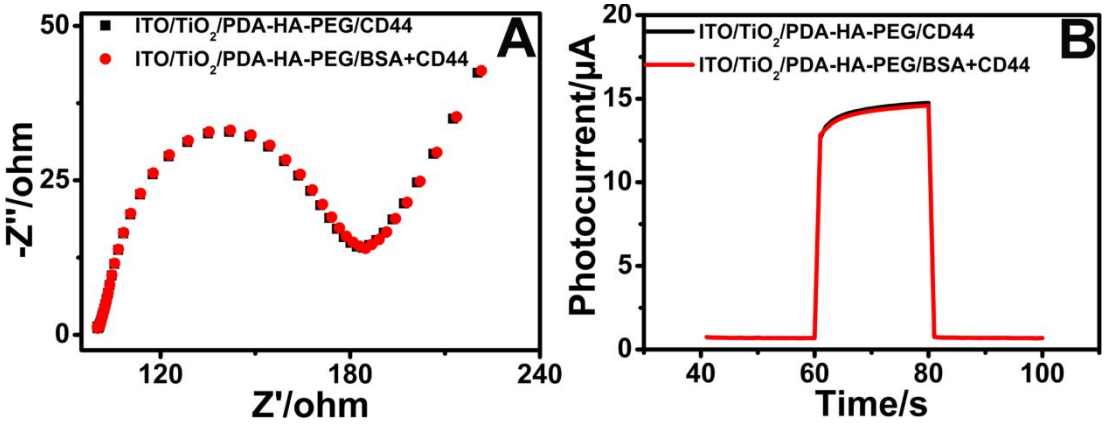

Figure 7. Nyquist plots of EIS (A) and photocurrent responses (B) of the ITO/TiO_2/PDA-HA-PEG electrodes soaking in CD44 solution (10 ng/mL) (black curve) and mixed solution (black curve) of CD44 (10 ng/mL) and BSA (0.5 mg/mL).

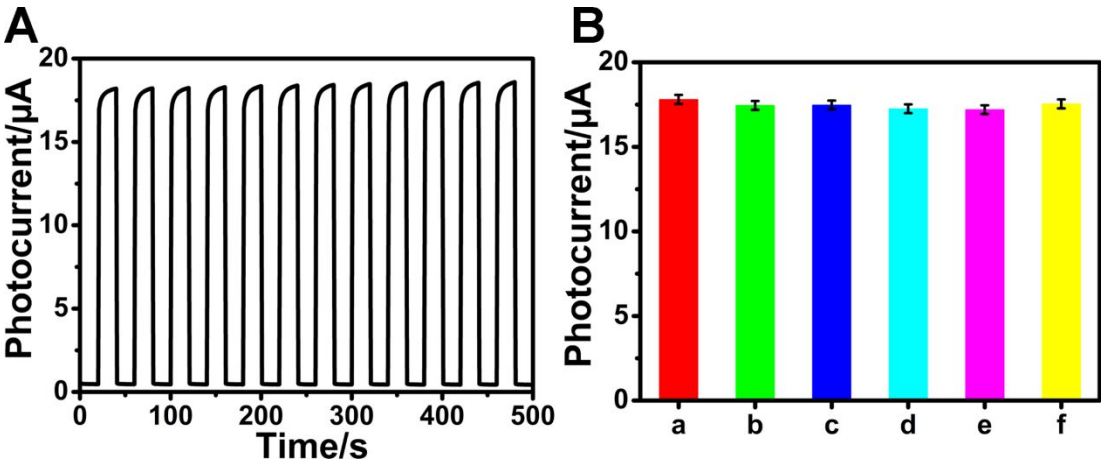

Figure 8. (A) The current stability test of 12 on/off lamp cycles of a PEC biosensor modified with CD44 (10 ng/mL). (B) The current reproducibility test of six PEC biosensors modified with CD44 (10 ng/mL).

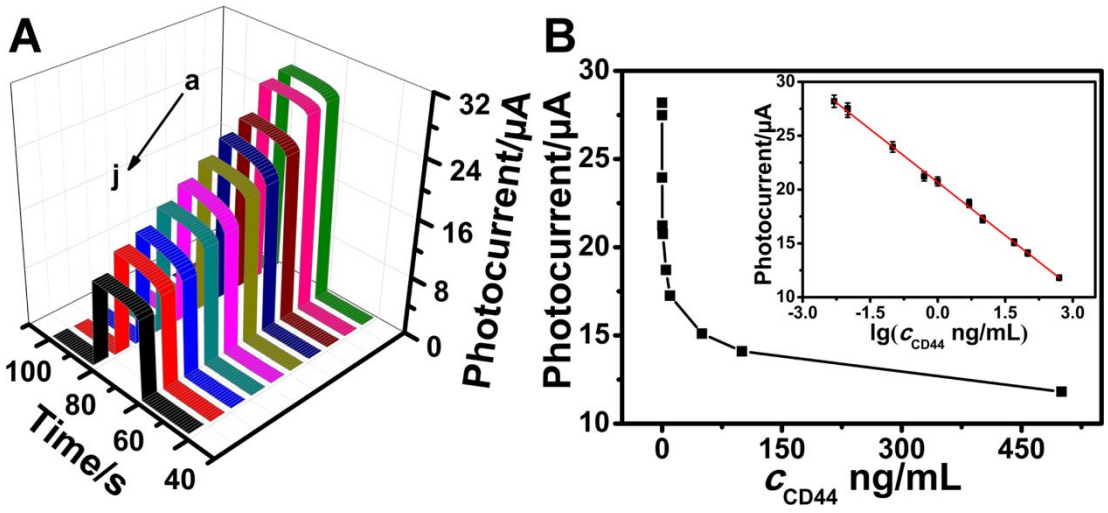

Figure 9. (A)Photocurrent responses of the PEC biosensor toward CD44 standard solutions with different concentrations: (a) 0.005，(b) 0.01, (c) 0.1, (d) 0.5, (e) 1, (f) 5, (g) 10, (h) 50, (i) 100, (j)500 ng/mL. (B) The changes in photocurrent versus different concentrations of CD44 ranging from 0.005 ng/mL to 500 ng/mL. Inset: the linear relationship between the change of photocurrent and the logarithm value of the CD44 concentration.

Table 1. Determination of CD44 in human serum sample.

Content of CD44 in the serum ($ng \cdot mL^{-1}$)	The addition content ($ng \cdot mL^{-1}$)	The average of the detected concentrations ($ng \cdot mL^{-1}$)	RSD (%, n=5)	Recovery (%, n=5)
250	30.00	280.14	2.04	100.50
	60.00	311.77	2.10	102.95
	90.00	342.49	2.35	102.77

Table of Contents

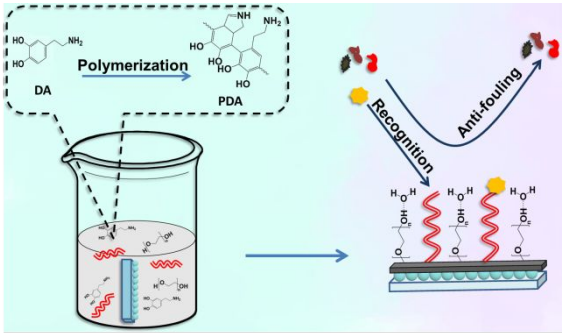

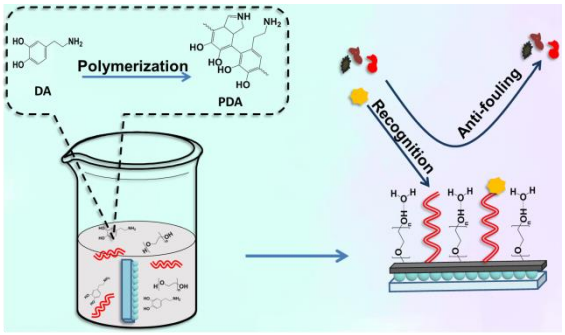

The serum level of soluble CD44 is directly associated with several clinic-pathological parameters of malignant diseases. The development of easy and cost-effective detection method for soluble CD44 is in great need for both diagnosis and treatment of cancers. In this work, a simple photoelectrochemical (PEC) method for sensitive detection of serum-soluble CD44 is proposed based on the construction of a hybrid anti-fouling coating on TiO_2 substrate. Hyaluronic acid (HA) and polyethylene glycol (PEG) are co-immobilized using a biomimetic one-step surface functionalization approach. The immobilized HA shows strong recognition abilities towards soluble CD44, and the synergistic anti-fouling effect achieved by the combination of PEG and HA improves the sensing specificity. Based on the inhibitory effect of CD44 recognition on the PEC signal of TiO_2 substrate, a PEC biosensor is developed with a wide response range and a low detection limit. The development of antibody-free biosensors may promote the application of soluble CD44 as a biomarker for diagnosis and treatment of malignant diseases.